Classification of 3-Degree-of-Freedom 3-UPU Translational Parallel Mechanisms Based on Constraint Singularity Loci Using Gröbner Cover

Xianwen Kong
School of Engineering and Physical Sciences,
Heriot-Watt University,
Edinburgh EH14 4AS, UK
e-mail: x.kong@hw.ac.uk

A 3-degree-of-freedom (DOF) 3-UPU translational parallel mechanism (TPM) is one of the typical TPMs. Despite comprehensive studies on 3-UPU TPMs in which the joint axes on the base and the moving platform are coplanar, only a few 3-UPU TPMs with skewed base and moving platform have been proposed, and the impact of link parameters on constraint singularity loci of such TPMs has not been systematically investigated. The advances in computing comprehensive Gröbner system (CGS) or Gröbner cover of parametric polynomial systems provide an efficient tool for solving this problem. This paper presents a systematic classification of 3-UPU TPMs with skewed base and moving platform based on constraint singularity loci. First, the constraint singularity equation of a 3-UPU TPM is derived. Using Gröbner cover, the 3-UPU TPMs are classified into 12 types. Finally, a novel 3-UPU TPM is proposed. Reconfiguration analysis shows that unlike most existing 3-UPU TPMs which can transit from a 3-DOF translational mode to two or more 3-DOF operation modes, the proposed 3-UPU TPM can only transit from a 3-DOF translational mode to one general 3-DOF operation mode. The singularity locus divides the workspace of this 3-UPU TPM into two constraint singularity-free regions. As a by-product, a 3-UPU parallel mechanism that the moving platform can undergo 3-DOF translation and 1-DOF infinitesimal rotation is revealed. This work provides a solid foundation for the design of 3-UPU TPMs and a starting point for the classification of 3-UPU parallel mechanisms. [DOI: 10.1115/1.4054307]

Keywords: translational parallel mechanism, constraint singularity, operation mode, reconfiguration analysis, Gröbner cover, parallel mechanism, theoretical kinematics

1 Introduction

A 3-UPU translational parallel mechanism (TPM, see Fig. 1) is one of the typical TPMs [1–3]. It is composed of a moving platform connected to the base by three UPU legs. Each UPU leg is a serial kinematic chain composed of a U joint, a P joint, and a U joint in sequence. For convenience, the R (revolute) joint within a U joint connected to the P joint is called an internal R joint, and the other R joint is called an external R joint. In each UPU leg, the axes of the two internal R joints and the P joint form a planar kinematic chain, which restrain the axes of the two external R joints to be coplanar.

Several types of 3-UPU TPMs have been proposed in the literature [2–9]. For the Tsai TPM [2], the axes of the R joints on the base or moving platform are coplanar. For the SNU TPM, the axes of the R joints on the base or moving platform are coplanar and intersect at the same point. In a 3-UPU TPM proposed in Ref. [5], the axes of the R joints on the base or moving platform are coplanar and two of them are parallel. Comprehensive studies on 3-UPU TPMs in which the joint axes on the base and the moving platform are coplanar [1–5,10–14] have been carried out. These TPMs have different constraint singularity loci and therefore different performances. It has been revealed that the SNU TPM has seven operation modes [11,12] and the Tsai TPM has five operation modes [13]. However, only a few 3-UPU TPMs with skewed base and moving platform [6–9] have been proposed. On a skewed base or moving platform, not all the joint axes of R joints are coplanar. In the 3-UPU TPMs with skewed base and moving platform [6,7], the axes of two R joints are parallel and the axis of the other R joint is perpendicular to the plane defined by these two parallel joint axes. In Ref. [7], a 3-UPU TPM with skewed based and platform was also proposed in which the axes of two R joints are coplanar and the axis of the third R joint is perpendicular to the plane defined by the axes of the first two R joints. In the 3-UPU (also called 3-RER) parallel mechanisms (PMs) presented in Ref. [8], the axes of all the R joints on the base or moving platform are perpendicular to each other and intersect at a common point. This 3-UPU PM has 15 operation modes, including four 3-DOF spatial translation modes. As pointed in Ref. [9], future research on 3-UPU TPMs should investigate 3-UPU TPMs with skewed base and moving platform and strategies to pass through constraint singularities.

This paper will investigate the impact of link parameters on constraint singularity loci of 3-UPU TPMs with skewed base and moving platform. This challenging issue has not been systematically investigated. Recent advances in computing comprehensive Gröbner system (CGS) or Gröbner cover of parametric polynomial systems (see, e.g., Refs. [15–17]) provide an efficient tool for tackling this problem. Gröbner cover [16] was used for solving the inverse kinematic analysis of planar robot, the kinematic analysis of planar mechanisms, and the identification of over-constrained planar mechanisms [18]. In Ref. [19], a systematic classification of 3-UPU PMs based on the type/number of operation modes was

The original version of this paper was presented at the ASME 2021 International Design Engineering Technical Conferences & Computers and Information in Engineering Conference, DETC2021-70059, Aug. 17–19, 2021.

Contributed by the Mechanisms and Robotics Committee of ASME for publication in the Journal of Mechanisms and Robotics. Manuscript received October 18, 2021; final manuscript received April 2, 2022; published online June 6, 2022. Assoc. Editor: Chin-Hsing Kuo.

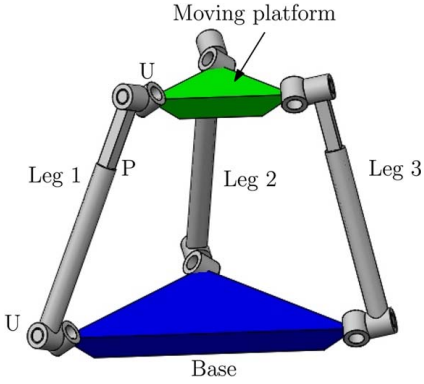

Fig. 1 A 3-UPU parallel mechanism

dealt with by using Gröbner cover and primary decomposition of ideals. The 3-UPU PMs in which the axes of all the R joints on the base or moving platform are parallel were classified into 13 types, each has two 4-DOF 3T1R operation modes and up to two more 3-DOF or other types of 4-DOF operation modes.

In Sec. 2, we will briefly illustrate how to solve parametric polynomial equations using Gröbner cover. The constraint equations of a 3-UPU PM are derived in Sec. 3. In Sec. 4, the constraint singularity equations of the 3-UPU TPM are formulated. The classification of 3-UPU TPMs is dealt with using Gröbner cover in Sec. 5. In Sec. 6, a novel 3-UPU TPM is proposed, and all the operation modes of the TPM are determined using the primary decomposition of ideals. Finally, conclusions are drawn.

2 A Note on Solving Parametric Polynomial Equations Using Gröbner Cover

Several algorithms (see, e.g., Refs. [15–17]) have been developed for computing CGS or Gröbner cover of parametric polynomial systems to obtain locally closed segments each of which accepts a set of functions that specialize to the reduced Gröbner basis for every point within the segment and each segment has different leading power products (lpp). The library for calculating Gröbner cover in Ref. [16], grobcov.lib, will be used in this paper to obtain the segments and the Gröbner bases associated with these segments.

In the following, the use of Gröbner cover will be illustrated by obtaining the well-known three cases of the intersection of two straight lines.

In order to reduce the parametric space without the loss of generality, let one straight line coincide with the X-axis and another line be in the general form of $ax+by+c=0$. The intersection of these two straight lines can then be obtained by solving the following set of parametric linear equations:

$$\begin{cases} ax+by+c=0 \\ y=0 \end{cases} \tag{1}$$

The ideal associated with the set of polynomial equations in Eq. (1) is

$$S=\langle ax+by+c,\, y\rangle$$

Using the following SINGULAR code, we can obtain the Gröbner cover in degree reverse lexicographical order (dp), which shows the three segments in the parametric space (a, b, c) together with the solutions in these segments as shown in Table 1. Each segment can be represented by one set or a combination of several sets via difference, $\setminus$, and union, $\bigcup$. The sets involved could be an n dimensional parametric set, $\mathbb{C}^n$, or a variety, V(*). The equations representing the three segments are listed in column 3, while the geometric characteristics of the two lines in different segments are given in column 4.

```
LIB "grobcov.lib";
ring R=(0,a,b,c),(x,y),dp;
ideal S=y, ax+by+c;
grobcov(S,"showhom",1);
```

Table 1 Intersections of two lines obtained using Gröbner cover

No.	Segment	Equation	Geometric characteristics	Intersection
S1	$\mathbb{C}^3 \setminus V(a)$	$a\neq 0$	Two lines are not parallel	$\begin{cases} y=0 \\ x=-c/a \end{cases}$
S2	$V(a) \setminus V(a, c)$	$\begin{cases} a=0 \\ c\neq 0 \end{cases}$	Two lines are parallel	$x\to\infty$
S3	$V(a, c)$	$\begin{cases} a=0 \\ c=0 \end{cases}$	Two lines coincide	$y=0$

Although the above solutions to Eq. (1) can be easily derived without using a computer, the Gröbner cover of more completed parametric polynomial systems cannot be obtained by hand calculations and the relevant algorithm/library [15–17] would be required.

It is noted that the use of degree reverse lexicographical order (dp) or lexicographical order (lp) may affect the CPU time required for calculating the Gröbner cover and even the Cröbner cover itself. It deserves to try both in calculating the Gröbner cover in order to better solve a kinematic problem. In this paper, the degree reverse lexicographical order (dp) would be used.

3 Constraint Equations of a 3-UPU Parallel Mechanism

In order to facilitate the classification of 3-UPU TPMs based on constraint singularity loci, $O-XYZ$ and $O_P-X_PY_PZ_P$ are attached to the base and moving platform (Fig. 2) in such a way that Y- and X-axes are along the joint axis of R joint on the base in leg 1 and the common perpendicular to the joint axes of R joints on the base in legs 1 and 2, respectively, and Y_P- and X_P-axes are along the joint axis of R joint on the moving platform in leg 1 and the common perpendicular to the joint axes of R joints on the moving platform in legs 1 and 2, respectively.

Let the joint centers of U joints on the base and moving platform be denoted by B_i ($i=1$, 2, and 3) and P_i ($i=1$, 2, and 3), respectively. $\mathbf{O}_P=\{x\ y\ z\}^T$ represents the position of O_P in the coordinate system $O-XYZ$. The coordinates of B_1, B_2, and B_3 in $O-XYZ$ are (0, 0, 0), $(n, 0, 0)$, and (u, v, w), respectively. The coordinates of P_1,

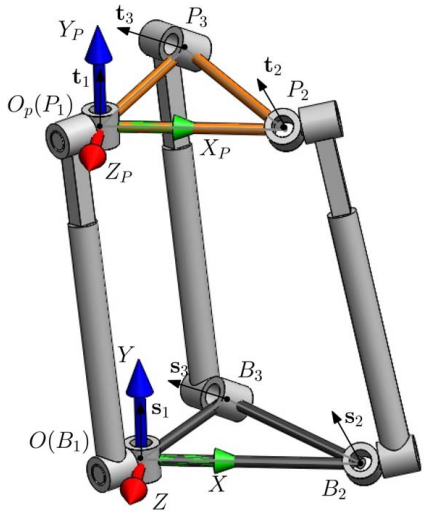

Fig. 2 Coordinate frames setup on a 3-UPU PM

P_2, and P_3 in $O_P - X_P Y_P Z_P$ are (0, 0, 0), (0, m, 0), and (r, s, t), respectively. Let $\mathbf{i}$, $\mathbf{j}$, and $\mathbf{k}$ denote the unit vectors along X-, Y-, and Z-axes, respectively. $\mathbf{w_1}$, $\mathbf{w_2}$, and $\mathbf{w_3}$ denote the unit vectors along X_P-, Y_P-, and Z_P-axes in the coordinate system $O - XYZ$. Let $\mathbf{s}_i$ ($i = 1$, 2, and 3) and $\mathbf{t}_i^{(P)}$ ($i = 1$, 2, and 3) denote the vectors along the axes of external R joints connected to the base in $O - XYZ$ and the vectors along the axes of external R joints connected to the moving platform in $O_P - X_P Y_P Z_P$. We have

$$\begin{cases} \mathbf{s}_1 = \mathbf{t}_1^{(P)} = \mathbf{j} \\ \mathbf{s}_2 = \mathbf{t}_2^{(P)} = \{0\ b\ c\}^T \\ \mathbf{s}_3 = \mathbf{t}_3^{(P)} = \{d\ e\ f\}^T \end{cases} \tag{2}$$

The position vectors of joint centers, B_i, of the three U joints on the base are

$$\begin{cases} \mathbf{r}_{B1} = \mathbf{0} \\ \mathbf{r}_{B2} = n\mathbf{i} \\ \mathbf{r}_{B3} = u\mathbf{i} + v\mathbf{j} + w\mathbf{k} \end{cases} \tag{3}$$

The position vectors of joint centers, P_i, of the three U joints on the moving platform are

$$\begin{cases} \mathbf{r}_{P1} = \mathbf{O}_P \\ \mathbf{r}_{P2} = \mathbf{O}_P + m\mathbf{w}_1 \\ \mathbf{r}_{P3} = \mathbf{O}_P + r\mathbf{w}_1 + s\mathbf{w}_2 + t\mathbf{w}_3 \end{cases} \tag{4}$$

In each UPU leg, the axes of the two external R joints are always coplanar due to the constraint imposed by the planar kinematic chain composed of the two internal R joints and P joint, i.e., the triple product of the two vectors along the axes of these two external R joints of leg i and vector $(\mathbf{r}_{Pi} - \mathbf{r}_{Bi})$ is equal to zero. Then, we obtain the set of constraint equations of leg i ($i = 1$, 2, and 3) as [8]

$$\mathbf{t}_i \times \mathbf{s}_i \cdot (\mathbf{r}_{Pi} - \mathbf{r}_{Bi}) = 0, \quad i = 1,\ 2 \text{ and } 3 \tag{5}$$

where $\mathbf{t}_i$ ($i = 1$, 2, and 3) denote the vectors along the axes of external R joints connected to the moving platform in $O - XYZ$ and can be calculated using

$$\begin{cases} \mathbf{t}_1 = \mathbf{w}_1 \\ \mathbf{t}_2 = b\mathbf{w}_1 + c\mathbf{w}_2 \\ \mathbf{t}_3 = d\mathbf{w}_1 + e\mathbf{w}_2 + f\mathbf{w}_3 \end{cases} \tag{6}$$

4 Constraint Singularity Equation of the 3-UPU Translational Parallel Mechanism

For a 3-UPU TPM, the axes of the two external R joints in each leg are parallel. For simplicity reasons, we set

$$\mathbf{t}_i = \mathbf{s}_i, \quad i = 1,\ 2 \text{ and } 3 \tag{7}$$

Substituting Eq. (7) into Eq. (5), we can readily prove that Eq. (5) is always true for the 3-UPU TPM.

In the 3-UPU TPM, each UPU leg imposes a constraint couple, which is perpendicular to the axes of all the R joints within the leg, on the moving platform. The direction of the constraint couple is readily obtained as

$$\mathbf{u}_i = \mathbf{s}_i \times (\mathbf{s}_i \times (\mathbf{r}_{Pi} - \mathbf{r}_{Bi})), \quad i = 1,\ 2 \text{ and } 3 \tag{8}$$

Therefore, constraint singularities happen if the three constraint couples are not linearly independent (or the three constraint couples are parallel to a common plane), i.e.,

$$\mathbf{u}_1 \times \mathbf{u}_2 \cdot \mathbf{u}_3 = 0 \tag{9}$$

In Ref. [5], the above constraint singularity of TPMs was called a rotational singularity, and the constraint singular condition was derived based on the Jacobin matrix of the 3-UPU TPM.

Substituting Eqs. (3), (4), and (2) into Eq. (8) and further substituting the resulted equation into Eq. (9), we obtain

$$\sum_{0 \le i,j,k, i+j+k \le 3} c_{i,j,k} x^i y^j z^k = 0 \tag{10}$$

where the coefficients $c_{i,j,k}$ are[1]

$$\begin{aligned} c_{300} &= 0 \\ c_{030} &= 0 \\ c_{003} &= bcdf \\ c_{210} &= cd(be + cf) \\ c_{201} &= -cd(bf - ce) \\ c_{120} &= -c(bd^2 + bf^2 - cef) \\ c_{021} &= -c^2 de \\ c_{102} &= c(bd^2 - bf^2 + cef) \\ c_{012} &= cd(be - cf) \\ c_{111} &= -2c^2 d^2 \\ &\cdots \end{aligned}$$

Equation (10) is generally a parametric cubic polynomial equation in x, y, and z representing the constraint singularity locus of the 3-UPU TPM. It is noted that the coefficient of each term with total degree 3 in x, y, and z in the singularity equation (Eq. (10)) only depends on the vectors along the R joint axes on the base or moving platform.

In the next section, we will investigate the classification of 3-UPU TPMs based on the constraint singularity loci by investigating how the link parameters affect the leading power products (lpp) of the constraint singularity equation using the Gröbner cover.

5 Classification of the 3-UPU Translational Parallel Mechanism Based on Constraint Singularity Locus Using Gröbner Cover

Using the library for calculating Gröbner cover [16], grobcov.lib, we can obtain the Gröbner cover of the ideal associated with Eq. (10). For the classification of 3-UPU TPMs, we only care about the segments within the Gröbner cover and the lpp of each segment. The segments for the 3-UPU TPM obtained are listed in Table 2.

Among the 16 segments, four segments, S3a, S3b, S3c, and S3d, lead to 3-UPU PMs that can undergo 1-DOF finite rotation (S3a) or 1-DOF infinitesimal rotation (S3b, S3c, and S3d) in addition to 3-DOF translation. In a type S3a 3-UPU PM, the axes of all the R joints on the moving platform (or the base) are parallel. Such a PM is in fact a 4-DOF 3T1R PM [20–22]. In a type S3b, S3c or S3d 3-UPU PM, one pair of legs meet the following conditions: (1) the axes of the R joints on the moving platform (or the base) are parallel and (2) the distance between the axes of the R joints on the moving platform is equal to that between the axes of the R joints on the base. Figure 3 shows the CAD model of a type S3b 3-UPU PM. In this 3-UPU PM, legs 1 and 2 meet the above conditions. Using Eq. (8), we can find that the constraint couples imposed on the moving platform by legs 1 and 2 are along the same direction $(\mathbf{j} \times (\mathbf{j} \times \mathbf{O}_P))$. The total constraints imposed on the moving platform by all the legs include two independent constraint couples, including one by leg 3 and one by legs 1 and 2. In addition to 3-DOF spatial translation, the moving platform can also undergo an infinitesimal rotation about a line perpendicular to the directions of the above two independent constraint couples in a general configuration. Such mechanisms are also called parallel mechanisms with

[1]The remaining coefficients not given here are functions of link parameters b, c, d, e, f, m, r, s, t, n, u, v, and w.

Table 2 Segments in the parametric space of the 3-UPU PM

Segment ID	lpp	Segment definition
S1	x^2y	$\mathbb{C}^{13} \setminus (V(be+cf) \bigcup V(d) \bigcup V(c))$
S2a	xz	$V(c) \setminus (V(m-n, c) \bigcup V(e, c) \bigcup V(d, c))$
S2b		$V(d, bf-ce) \setminus (V(c, d, f) \bigcup V(d, bf-ce, et-ew-fs+fv, bt-bw-cs+cv))$
(S3a)	0	$V(f, d, c)$
(S3b)		$V(m-n, c)$
(S3c)		$V(t-w, r-u, f, d)$
(S3d)		V_{3d}
S4a	yz	$V(d, c) \setminus (V(m-n, d, c) \bigcup V(f, d, c))$
S4b		$V(e, c) \setminus V(m-n, e, c)$
S4c		$V(t-w, f, d) \setminus (V(r-u, t-w, f, d) \bigcup V(c, t-w, f, d))$
S4d		$V(et-ew-fs+fv, d, bt-bw-cs+cv, bf-ce) \setminus (V_{3d} \bigcup (c, t-w, f, d))$
S5a	xy^2	$V(d) \setminus (V(d, bf-ce) \bigcup V(d, f) \bigcup V(d, c))$
S5b		$V(be+cf) \setminus (V(f, b) \bigcup (e, c))$
S6	xy	$V(f, d) \setminus (V(t-w, f, d) \bigcup (c, f, d))$
S7	xyz	$V(b, e, f)$
S8	x^2z	$V(b, f) \setminus (V(b, e, f) \bigcup (b, d, f))$

Note: $V_{3d} = V(m-n-r+u, et-ew-fs+fv, d, bt-bw-cs+cv, bf-ce)$

mixed instantaneous and full-cycle mobility [23] or shaky mechanisms [24]. Unlike most shaky mechanisms in the literature (see, for instance, Refs. [23–25]), the 1-DOF infinitesimal rotation of the above PM could not be eliminated by locking one of its joints. The potential application of this PM in assembly where compliance is required deserves further investigation.

Discarding these four segments and putting these four segment numbers into brackets in Table 2, the parameter space of the 3-UPU TPM is divided into 12 segments. Therefore, the 3-UPU TPM can be classified into 12 types (Table 2): S1, S2a, S2b, S4a, S4b, S4c, S4d, S5a, S5b, S6, S7, and S8.

From Table 2, the geometric characteristics of the 12 types of 3-UPU TPMs can be revealed as follows.

(1) In a Type S2a, S2b, S4a, S4b, S4c, S4d, or S6 3-UPU TPM, the axes of two R joints on the base are parallel. The total degree of lpp in x, y, and z for these eight types of 3-UPU TPM is 2. Therefore, the constraint singularity loci of these 3-UPU TPMs are of degree 2.
(2) In a Type S5a 3-UPU TPM, the joint axes of all the three R joints on the base are parallel to one plane. The constraint singularity loci of these 3-UPU TPMs are of degree 3 with a lpp of xy^2.
(3) In a Type S7 3-UPU TPM, the joint axes of all the three R joints on the base are perpendicular to each other. The constraint singularity loci of these 3-UPU TPMs are of degree 3 with a lpp of xyz.
(4) In a Type S5b or S8 3-UPU TPM, the joint axes of two R joints on the base are perpendicular to each other. The constraint singularity loci of these 3-UPU TPMs are of degree 3 with a lpp of xy^2 for Type S5b or a lpp of x^2z for Type S8.
(5) In a Type S1 3-UPU TPM, the joint axes of any two R joints on the base are neither perpendicular nor parallel to each other, and the joint axes of all the three R joints on the base are not parallel to one plane. The constraint singularity locus of the Type S1 3-UPU TPM is of degree 3 with a lpp of x^2y.

It is noted that the 3-UPU TPM with planar base and platform and a pair of R joints with parallel axes [5] falls in Type S2a or S6. The 3-UPU TPMs with skewed base and platform and a pair of R joints with parallel axes [6,7] are special cases of Type S4a, S4b, S4c, or S4d. The Tsai TPM [2], SNU TPM [11,12], and a general 3-UPU TPM with planar base and platform [5] fall in Type S5a. The reconfigurable 3-UPU PM in its 3-DOF translation mode [8] is a specific case of Type S7. The 3-UPU TPM with skewed based and platform [7], in which the axes of two R joints are coplanar and the axis of the third R joint is perpendicular to the plane defined by the axes of the first two R joints, is a special case of Type S5b or S8. A general 3-UPU TPM with skewed base and platform (see [9] for instance), which has not been well defined before, can be defined as a Type S1 UPU TPM.

6 Operation Mode Analysis of a Novel 3-UPU Translational Parallel Mechanism

In this section, we will analyze all the operation modes of a novel 3-UPU TPM, which is a general case of Type S7 3-UPU TPM, to reveal its characteristics.

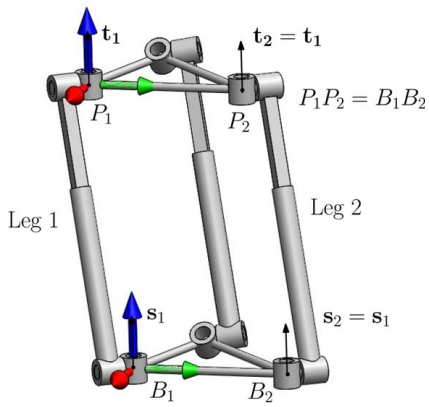

Fig. 3 A Type S3b 3-UPU PM that the moving platform undergoes 3-DOF (finite) translation and 1-DOF infinitesimal rotation

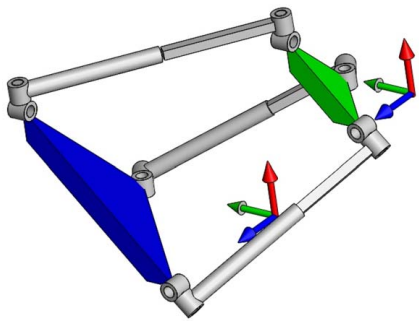

Fig. 4 A novel 3-UPU TPM

6.1 Description of a Novel 3-UPU Translational Parallel Mechanism. The link parameters of a novel Type S7 3-UPU TPM (Fig. 4) are: $b=0$, $c=1$, $d=1$, $e=0$, $f=0$, $m=1$, $r=1$, $s=1$, $t=1$, $n=2$, $u=2$, $v=2$, $w=2$. In this 3-UPU TPM, the joint axes of the R joints on the base are along the *Y*-, *Z*-, and *X*-axes, respectively. Unlike the 3-UPU TPM in Ref. [8], the joint axes of the R joints on the base do not intersect with each other.

From Eq. (10), the constraint singularity equation of this 3-UPU TPM is

$$-2xyz + xy + xz + yz - z = 0 \tag{11}$$

From its constraint singularity locus (Fig. 5), we can observe that the workspace of this novel TPM is divided into two constraint singularity-free regions, while for most existing 3-UPU TPMs, the workspace is divided into four or more constraint singularity-free regions [5–9].

6.2 Constraint Equations. Using Euler parameters to represent the orientation of the moving platform, the unit vectors along X_P- and Y_P-, and Z_P-axes are [8]

$$\mathbf{w}_1 = \begin{Bmatrix} e_0^2 + e_1^2 - e_2^2 - e_3^2 \\ 2(e_1e_2 + e_0e_3) \\ 2(e_1e_3 - e_0e_2) \end{Bmatrix} \tag{12}$$

$$\mathbf{w}_2 = \begin{Bmatrix} 2(e_1e_2 - e_0e_3) \\ e_0^2 - e_1^2 + e_2^2 - e_3^2 \\ 2(e_2e_3 + e_0e_1) \end{Bmatrix} \tag{13}$$

$$\mathbf{w}_3 = \begin{Bmatrix} 2(e_1e_3 + e_0e_2) \\ 2(e_2e_3 - e_0e_1) \\ e_0^2 - e_1^2 - e_2^2 + e_3^2 \end{Bmatrix} \tag{14}$$

where

$$e_0^2 + e_1^2 + e_2^2 + e_3^2 = 1 \tag{15}$$

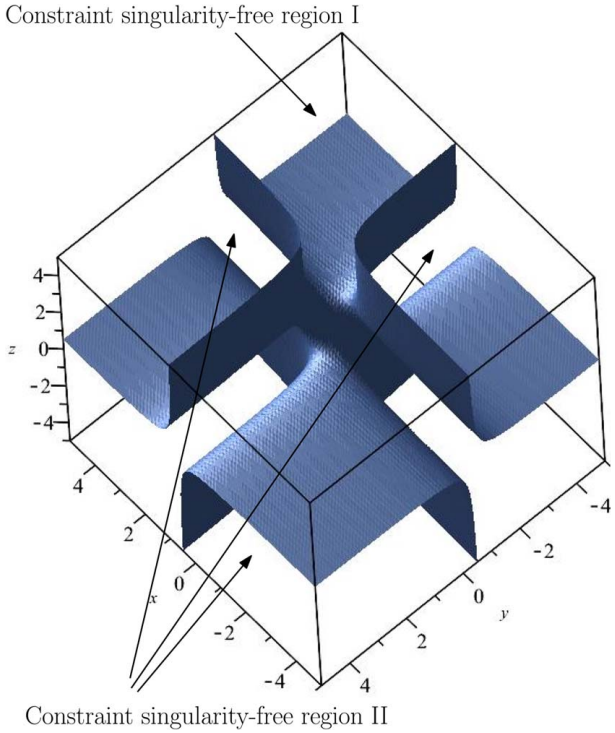

Fig. 5 Constraint singularity locus of the 3-UPU TPM

Substituting Eqs. (12)–(14) into Eq. (6) and the resulted equation further into Eq. (5), we obtain the constraint equations of the novel 3-UPU TPM as

$$\begin{cases} (e_0e_1 + e_2e_3)x + z(e_0e_3 - e_1e_2) = 0 \\ ((x-1)e_1 + ye_2)e_0 - (-ye_1 + e_2(x-3))e_3 = 0 \\ ((y-1)e_2 + e_3(z-1))e_0 - \\ ((-z+3)e_2 + e_3(y-3))e_1 = 0 \end{cases} \tag{16}$$

Using the primary decomposition of ideals, one can calculate the positive dimensional solutions to polynomial constraint equations of a PM. Each positive solution is associated with one operation mode of the PM [8,12,19,26]. For this 3-UPU TPM, five operation modes (Table 3) can be obtained.

In each operation mode, the DOF of 3-UPU TPM can be readily obtained by calculating the difference between the number of variables (x, y, z, e_0, e_1, e_2, and e_3) and the number of independent constraint equations including Eq. (15). For example, the DOF in the operation mode associate with the first four operation modes is 3 ($=7-4$). One can also obtain the DOF of the 3-UPU TPM in operation mode V which has a set of complicated constraint equations by calculating the Hilbert dimension of the ideal associated with the constraint equations using a computer algebra system. Using the kinematic interpretation of 15 cases of Euler parameter quaternions [8], the motion characteristics of the moving platform of the PM in the first four operation modes can be readily obtained. For example, the motion of the moving platform in operation mode IV is a 3-DOF translation mode (Fig. 6(*a*)).

The motion of the 3-UPU PM in operation mode V (Fig. 6(*b*)) is very complicated as described using Eqs. (17) and (15)

$$\begin{cases} f_1 = 0 \\ f_2 = 0 \\ \cdots \\ f_{13} = 0 \end{cases} \tag{17}$$

where $f_1 = x^2ye_1e_3 - 3x^2e_1e_3 - xyze_1^2 + xyze_3^2 + 3/2xye_1^2 - 2xye_1e_3 - 1/2xye_3^2 + 3/2xze_1^2 - 3/2xze_3^2 + 6xe_1e_3 + y^3e_1e_3 - y^2ze_0e_3 - y^2ze_1e_2 - 1/2y^2e_0e_1 + 1/2y^2e_0e_3 + 3/2y^2e_1e_2 - 3y^2e_1e_3 + 3/2y^2e_2e_3 - yz^2e_1e_3 + 3/2yze_0e_3 + 1/2yze_1^2 + 3/2yze_1e_2 + 2yze_1e_3 - 3/2yze_3^2 + ye_0e_1 - 1/2ye_0e_3 - 3/2ye_1e_2 + ye_1e_3 - 3ye_2e_3 + 1/2ze_0e_3 - 3/2ze_1^2 +$

Table 3 Five operation modes of a novel 3-DOF 3-UPU PM

Operation mode	Equation (15)
I: 3-DOF translation	$\begin{cases} e_0 = 0 \\ e_1 = 0 \\ e_2 = 0 \end{cases}$
II: 3-DOF translation	$\begin{cases} e_0 = 0 \\ e_1 = 0 \\ e_3 = 0 \end{cases}$
III: 3-DOF translation	$\begin{cases} e_0 = 0 \\ e_2 = 0 \\ e_3 = 0 \end{cases}$
IV: 3-DOF translation	$\begin{cases} e_1 = 0 \\ e_2 = 0 \\ e_3 = 0 \end{cases}$
V: General 3-DOF motion	Eq. (17)

$1/2ze_1e_2+9/2ze_3^2-1/2e_0e_2-1/2e_0e_3-3/2e_1e_2+3/2e_1e_3, f_2=x^2$
$ze_0e_3-x^2e_0e_3-xyze_0^2+xyze_3^2+1/2xye_0^2-1/2xye_3^2+1/2xze_0^2-2xz$
$e_0e_3-3/2xze_3^2+2xe_0e_3-y^2ze_0e_3+1/2yze_0^2+2yze_0e_3-3/2yze_3^2$
$-z^3e_1e_2+1/2z^2e_0e_1+1/2z^2e_0e_2+1/2z^2e_0e_3+7/2z^2e_1e_2-3/2z^2$
$e_1e_3+3/2z^2e_2e_3-1/2ze_0^2-ze_0e_1-ze_0e_2-ze_0e_3-3ze_1e_2+3ze_1$
$e_3-3ze_2e_3+9/2ze_3^2, f_3=x^2ze_1e_2-3x^2e_1e_2-xyze_1^2+xyze_2^2+$
$3/2xye_1^2-3/2xye_2^2+3/2xze_1^2-2xze_1e_2-1/2xze_2^2+6xe_1e_2-y^2z$
$e_1e_2+1/2yze_1^2+2yze_1e_2-3/2yze_2^2-z^3e_0e_3-1/2z^2e_0e_1+1/2z^2e_0$
$e_2+5/2z^2e_0e_3+3/2z^2e_1e_2-3/2z^2e_1e_3-3/2z^2e_2e_3+ze_0e_1-ze_0$
$e_2-ze_0e_3-3/2ze_1^2-3ze_1e_2+3ze_1e_3+3/2ze_2^2+3ze_2e_3, f_4=$
$xye_1^2e_3-xze_1^2e_2+3xe_1^2e_2-3xe_1^2e_3+y^2e_1e_2e_3-yze_1e_2^2+yze_1e_3^2$
$-1/2ye_1^2e_3+3/2ye_1e_2^2-2ye_1e_2e_3-1/2ye_1e_3^2+3/2ye_2^2e_3-z^2e_1e_2e_3$
$+1/2ze_1^2e_2+1/2ze_1e_2^2+2ze_1e_2e_3-3/2ze_1e_3^2+3/2ze_2e_3^2-3/2e_1^2e_2+$
$3/2e_1^2e_3-3/2e_2^2e_3-3/2e_2e_3^2, f_5=xye_1e_3^2-xze_0e_3^2+xe_0e_3^2-3xe_1e_3^2$
$-y^2e_0e_1e_3+yze_0^2e_3-yze_1^2e_3+1/2ye_0^2e_1-1/2ye_0^2e_3+2ye_0e_1e_3+$
$3/2ye_1^2e_3-3/2ye_1e_3^2+z^2e_0e_1e_3-1/2ze_0^2e_3+1/2ze_0e_1^2-2ze_0e_1e_3+$
$3/2ze_0e_3^2+3/2ze_1^2e_3-1/2e_0^2e_1-3/2e_0e_1^2-3/2e_0e_3^2+9/2e_1e_3^2, f_6=$
$xze_0^2e_3^2-xe_0^2e_3^2+y^2e_0^2e_1e_3+y^2e_1e_3^3-yze_0^3e_3-2yze_1e_2e_3^2-1/2ye_0^3e_1+$
$1/2ye_0^3e_3-2ye_0^2e_1e_3+ye_0e_1e_3^2+1/2ye_0e_3^3+3ye_1e_2e_3^2-4ye_1e_3^3$
$+3/2ye_2e_3^3+z^2e_1e_2^2e_3+1/2ze_0^3e_3-1/2ze_0^2e_1e_2-3/2ze_0^2e_3^2-$
$3/2ze_0e_1^2e_2-ze_0e_1e_2e_3-1/2ze_0e_2^2e_3-1/2ze_0e_2e_3^2-1/2ze_0e_3^3-$
$3ze_1e_2^2e_3+4ze_1e_2e_3^2-3/2ze_2^2e_3^2+1/2e_0^3e_1+3/4e_0^2e_1^2+3/4e_0^2e_1e_2$
$+3/4e_0^2e_1e_3+3/2e_0^2e_3^2+9/4e_0e_1^2e_2-9/4e_0e_1^2e_3+3/2e_0e_1e_2e_3-$
$3e_0e_1e_3^2+3/4e_0e_2^2e_3-1/4e_0e_2e_3^2-e_0e_3^3+9/4e_1e_2^2e_3-21/4e_1e_2e_3^2$
$+3e_1e_3^3+9/4e_2^2e_3^2-9/2e_2e_3^3, f_7=xze_1^2e_2^2-3xe_1^2e_2^2-y^2e_1^3e_3-$
$y^2e_1e_2^2e_3+yze_1e_2^3-2yze_1e_2e_3^2+1/2ye_0e_1^3-3/2ye_1^3e_2+4ye_1^3e_3-$
$ye_1^2e_2e_3-3/2ye_1e_2^3+2ye_1e_2^2e_3+ye_1e_2e_3^2-3/2ye_2^3e_3+z^2e_0^2e_1e_3+$
$2z^2e_1e_2^2e_3+1/2ze_0^2e_1^2-1/2ze_0^2e_1e_2-ze_0^2e_1e_3-3/2ze_0e_1^2e_2-ze_0e_1^2e_3$
$-ze_0e_1e_2e_3-1/2ze_0e_2^2e_3-1/2ze_0e_2e_3^2+1/2ze_1^3e_2-1/2ze_1^2e_2^2-1/2z$
$e_1e_3^2-4ze_1e_2^2e_3+3ze_1e_2e_3^2-3ze_2^2e_3^2-1/4e_0^2e_1^2+1/4e_0^2e_1e_2+1/4e_0^2$
$e_1e_3-3/2e_0e_1^3+7/4e_0e_1^2e_2+1/4e_0e_1^2e_3+1/2e_0e_1e_2e_3+1/4e_0e_2^2e_3+$
$1/4e_0e_2e_3^2+3e_1^3e_2-3e_1^3e_3+3/2e_1^2e_2^2+3e_1^2e_2e_3+3/4e_1e_2^2e_3-3/4e_1$
$e_2e_3^2+3/2e_2^3e_3+9/4e_2^2e_3^2, f_8=xe_0e_1+ye_1e_3-ze_1e_2-1/2e_0e_1+$
$1/2e_0e_2+1/2e_0e_3+3/2e_1e_2-3/2e_1e_3+3/2e_2e_3, f_9=xe_2e_3-$
$ye_1e_3+ze_0e_3+1/2e_0e_1-1/2e_0e_2-1/2e_0e_3-3/2e_1e_2+3/2e_1e_3$
$-3/2e_2e_3, f_{10}=ye_0e_1^2e_3+ye_1e_2e_3^2-ze_0^2e_1e_3-ze_1e_2^2e_3-1/2e_0^2e_1^2+$
$1/2e_0^2e_1e_2+1/2e_0^2e_1e_3+3/2e_0e_1^2e_2-3/2e_0e_1^2e_3+e_0e_1e_2e_3+$
$1/2e_0e_2^2e_3+1/2e_0e_2e_3^2+3/2e_1e_2^2e_3-3/2e_1e_2e_3^2+3/2e_2^2e_3^2, f_{11}=$
$ye_0e_2-ye_1e_3+ze_0e_3+ze_1e_2-e_0e_2-e_0e_3-3e_1e_2+3e_1e_3, f_{12}=$
$ye_1^2e_3^2+ye_1e_2^2e_3^2-ze_0^2e_1e_2e_3-ze_0e_1^2e_3^2-ze_1^3e_2e_3-ze_1e_2^3e_3-$
$1/2e_0^2e_1^2e_2+1/2e_0^2e_1e_2^2+1/2e_0^2e_1e_2e_3+3/2e_0e_1^2e_2^2-1/2e_0e_1^2e_2e_3$
$+e_0e_1^2e_3^2+e_0e_1e_2^2e_3+1/2e_0e_2^3e_3+1/2e_0e_2^2e_3^2+3e_1^3e_2e_3-3e_1^3e_3^2+$
$3/2e_1e_2^3e_3-3/2e_1e_2^2e_3^2+3/2e_2^3e_3^2$, and $f_{13}=ze_0^3e_1e_2e_3+ze_0e_1^3e_2e_3$
$+ze_0e_1e_3^3e_3+ze_0e_1e_2e_3^3+1/2e_0^3e_1^2e_2-1/2e_0^3e_1e_2^2-1/2e_0^3e_1e_2e_3-$
$1/2e_0^2e_1^3e_3-3/2e_0^2e_1^2e_2^2+e_0^2e_1^2e_2e_3-1/2e_0^2e_1^2e_3^2-e_0^2e_1e_2^2e_3-1/2e_0^2e_2^3e_3$
$-1/2e_0^2e_2^2e_3^2-3/2e_0e_1^3e_2e_3+3/2e_0e_1^3e_3^2+e_0e_1^2e_2e_3^2-3/2e_0e_1e_2^3e_3$
$+e_0e_1e_2^2e_3^2-1/2e_0e_1e_2e_3^3-3/2e_0e_2^3e_3^2-3/2e_1^2e_2^2e_3^2+3/2e_1^2e_2e_3^3+$
$3/2e_1e_2^2e_3^3$.

Considering that the reference configuration of the 3-UPU TPM is in operation mode IV, we mainly care about the transition configurations between operation modes IV and the remaining four operation modes in this paper. Solving the set of equation composed of equations associated with operation modes IV and V, we obtain the same equation as Eq. (10), which is the equation of constraint singularities of the 3-UPU TPM. This means that the transition configurations between operation modes IV and V are the constraint singular configurations of the 3-UPU TPM. From Eq. (15), one obtains that e_0, e_1, e_2, and e_3 cannot vanish at the same time. Therefore, there is no common configuration between operation mode IV and any of operation modes I to III, and the 3-UPU TPM cannot transit from operation mode IV to any of operation modes I to III directly.

Some of the 3-UPU TPMs in the literature can transit to more than one operation mode other than the 3-DOF translation mode at a constraint singular configuration [8,11–13].

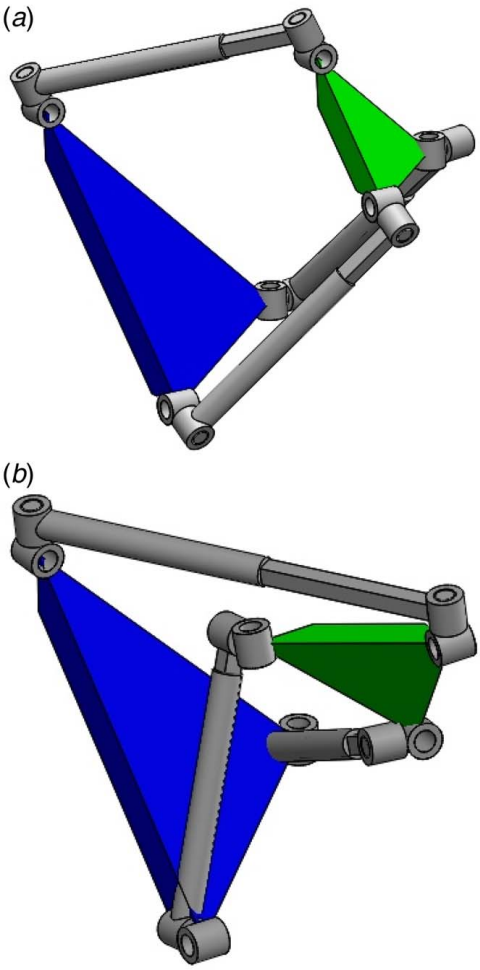

Fig. 6 A novel 3-UPU PM in (*a*) 3-DOF translation mode IV and (*b*) 3-DOF general operation mode V

7 Conclusions

The 3-UPU TPM has been classified into 12 types based on the singularity loci using the Gröbner cover. The analysis of a novel 3-UPU TPM has shown that besides the 3-DOF translational operation modes, the 3-UPU TPM may have a 3-DOF general operation mode. Unlike most existing 3-UPU TPMs for which the workspace is divided into four or more constraint singularity-free regions, the workspace of this 3-UPU TPM is divided into two constraint singularity-free regions.

This work is a step forward in the design of the 3-UPU TPMs and classification of 3-UPU PMs. The 3-UPU PM that the moving platform can undergo 3-DOF translation and 1-DOF infinitesimal rotation in a general configuration and its potential application in assembly also deserve further investigation.

Acknowledgment

The author would like to thank the Engineering and Physical Sciences Research Council (EPSRC), United Kingdom, for the support (Grant No. EP/T024844/1). For the purpose of open access, the author has applied a Creative Commons Attribution (CC BY) licence (where permitted by UKRI, "Open Government Licence" or "Creative Commons Attribution No-derivatives (CC BY-ND) licence" may be stated instead) to any Author Accepted Manuscript version arising.

Conflict of Interest

There are no conflicts of interest.

Data Availability Statement

The authors attest that all data for this study are included in the paper.

References

[1] Hunt, K. H., 1973, "Constant-Velocity Shaft Couplings: A General Theory," J. Eng. Ind., **95**(2), pp. 455–464.

[2] Tsai, L.-W., 1996, "Kinematics of a Three-DOF Platform With Three Extensible Limbs," *Recent Advances in Robot Kinematics*, J. Lenarčič, and V. Parenti-Castelli, eds., Springer Netherlands, Dordrecht, pp. 401–410.

[3] Parenti-Castelli, V., and Bubani, F., 1999, "Singularity Loci and Dimensional Design of a Translational 3-DOF Fully-Parallel Manipulator," *Advances in Multibody Systems and Mechatronics*, A. Kecskeméthy, M. Schneider, and C. Woernle, eds., Institut für Mechanik und Getriebelehre, Technische Universität Graz, Graz, Austria, pp. 319–331.

[4] Di Gregorio, R., and Parenti-Castelli, V., 1999, "Influence of the Geometric Parameters of the 3-UPU Parallel Mechanism on the Singularity Loci," Proceedings of the International Workshop on Parallel Kinematic Machines (PKM'99), Milan, Italy, Nov. 30, pp. 79–86.

[5] Di Gregorio, R., and Parenti-Castelli, V., 2002, "Mobility Analysis of the 3-UPU Parallel Mechanism Assembled for a Pure Translational Motion," ASME J. Mech. Des., **124**(2), pp. 259–264.

[6] Hu, B., Yao, Y., and Wu, P., 2013, "A Comparison Study of Two 3-UPU Translational Parallel Manipulators," Int. J. Adv. Robot. Syst., **10**(4), pp. 188–201.

[7] Chebbi, A., and Parenti-Castelli, V., 2013, "The Potential of the 3-UPU Topology for Translational Parallel Manipulators and a Procedure to Select the Best Architecture for a Given Task," Rom. J. Tech. Sci. – Appl. Mech., **58**(2), pp. 5–32.

[8] Kong, X., 2014, "Reconfiguration Analysis of a 3-DOF Parallel Mechanism Using Euler Parameter Quaternions and Algebraic Geometry Method," Mech. Mach. Theory, **74**, pp. 188–201.

[9] Di Gregorio, R., 2020, "A Review of the Literature on the Lower-Mobility Parallel Manipulators of 3-UPU Or 3-URU Type," Robotics, **9**(1), p. 5.

[10] Kong, X., 2017, "Standing on the Shoulders of Giants: A Brief Note From the Perspective of Kinematics," Chin. J. Mech. Eng., **30**(1), pp. 1–2.

[11] Zlatanov, D., Bonev, I. A., and Gosselin, C. M., 2002, "Constraint Singularities As C-Space Singularities," *Advances in Robot Kinematics: Theory and Applications*, Lenarčič, F., and Thomas, J., eds., Springer Netherlands, Dordrecht, pp. 183–192.

[12] Walter, D. R., Husty, M. L., and Pfurner, M., 2009, "A Complete Kinematic Analysis of the SNU 3-UPU Parallel Robot," *Interactions of Classical and Numerical Algebraic Geometry*, D. J. Bates, G. M. Besana, and S. Di Rocco, eds., AMS, Providence, RI, pp. 331–346.

[13] Husty, M. L., and Schröcker, H.-P., 2013, "Kinematics and Algebraic Geometry," *21st Century Kinematics*, J. M. McCarthy, ed., Springer, London, pp. 85–123.

[14] Zlatanov, D., and Gosselin, C. M., 2004, "On the Kinematic Geometry of 3-RER Parallel Mechanisms," Proceedings of the 11th IFToMM World Congress in Mechanism and Machine Science, Tianjin, China, Apr. 1–4, Vol. 1, pp. 226–230.

[15] Montes, A., and Wibmer, M., 2010, "Gröbner Bases for Polynomial Systems With Parameters," J. Symb. Comput., **45**(12), pp. 1391–1425.

[16] Montes, A., and Wibmer, M., 2014, "Software for Discussing Parametric Polynomial Systems: The Gröbner Cover," *Mathematical Software – ICMS 2014*, H. Hong, C. Yap, ed., Springer, Berlin/Heidelberg, pp. 406–413.

[17] Hashemi, A., and Darmian, M., 2017, "Computing Comprehensive Gröbner Systems: A Comparison of Two Methods," Comput. Sci. J. Moldova, **25**(3), pp. 278–302.

[18] Arikawa, K., 2019, "Kinematic Analysis of Mechanisms Based on Parametric Polynomial System: Basic Concept of a Method Using Gröbner Cover and Its Application to Planar Mechanisms," ASME J. Mech. Rob., **11**(2), p. 020906.

[19] Kong, X., 2021, "Classification of a 3-RER Parallel Manipulator Based on the Type and Number of Operation Modes," ASME J. Mech. Rob., **13**(2), p. 021013.

[20] Huang, Z., Li, Q., and Ding, H., 2012, *Theory of Parallel Mechanisms*, Springer, Dordrecht, The Netherlands.

[21] Yang, T.-L., Liu, A., Shen, H., Hang, L., Luo, Y., and Jin, Q., 2018, *Topology Design of Robot Mechanisms*, Springer, Singapore.

[22] Kong, X., and Gosselin, C., 2007, *Type Synthesis of Parallel Mechanisms*, Springer, Dordrecht, The Netherlands.

[23] Kong, X., and Gosselin, C. M., 2005, "Mobility Analysis of Parallel Mechanisms Based on Screw Theory and the Concept of Equivalent Serial Kinematic Chain," 29th Mechanisms and Robotics Conference, Parts A and B of International Design Engineering Technical Conferences and Computers and Information in Engineering Conference, Long Beach, CA, Sept. 24–28, Vol. 7, pp. 911–920.

[24] Muller, A., 2016, "Local Kinematic Analysis of Closed-Loop Linkages – Mobility, Singularities, and Shakiness," ASME J. Mech. Rob., **8**(4), p. 041013.

[25] Kong, X., and Müller, A., 2018, "A Single-Loop 7R Spatial Mechanism That Has Three Motion Modes With the Same Instantaneous DOF But Different Finite DOF," 42nd Mechanisms and Robotics Conference of International Design Engineering Technical Conferences and Computers and Information in Engineering Conference, Vol. 5B, Paper No. V05BT07A070.

[26] Nurahmi, L., Caro, S., Wenger, P., Schadlbauer, J., and Husty, M., 2016, "Reconfiguration Analysis of a 4-RUU Parallel Manipulator," Mech. Mach. Theory, **96**, pp. 269–289.